MODELLING CYLINDERS AND CABLES MOTION INDUCED BY VORTEX VIBRATION

Paulo Fernando Villafañe Garcia, pfvg@petrobras.com.br
Petróleo Brasileiro S.A., Universidade Petrobras, Escola de Ciências e Tecnologias de Exploração e Produção
Av. Tancredo Neves, Edf. Civil Trade, Caminho das Árvores, 41820-020, Salvador – BA – Brazil

Francisco Ricardo da Cunha, frcunha@uol.com.br
Universidade de Brasília, Faculdade de Tecnologia, Departamento de Engenharia Mecânica
Campus Universitário Darcy Ribeiro, 70910-900, Brasília – DF – Brazil

Abstract. *In this article we derive the governing differential equations for modelling the unsteady bidimensional motion of a cylinder suspended by four parallel springs and a cable with pinned ends with both structures under the effects of a cross-flow. A dimensional analysis is used to obtain the level of greatness and influence of the variables involved in the governing equations of a wind-vortex-induced vibratory motion. The relevant physical parameters of the fluid-structure interaction problem examined are the Reynolds number, the anisotropic ratio and the dimensionless frequency. The situations of short and long cables are also identified by means of the dimensional analysis. The nondimensionalized governing equation of the cylinder vibration problem is solved by using perturbation methods and time-step adaptive numerical solution. An analysis of several nonlinear responses obtained is carried out in the frequency domain. Results of the transversal displacement are presented for different Reynolds numbers, anisotropic ratios and frequencies. In addition, the nondimensionalized governing equation of the cable vibration problem is solved analytically, assuming the self-damping coefficient to be constant in time. The same governing equation is solved numerically using the finite difference method. A comparison between the numerical and analytical results shows good agreement.*

Keywords*: vortex-induced vibration, perturbation method, finite difference method, nonlinear frequency response*

1. INTRODUCTION

When a fluid flows around a cylinder-shaped body, vortexes of intercalated configuration downstream the body are formed. To this phenomenon is given the name of vortex shedding (Batchelor, 1967). The vortexes are presented alternatingly with circulations in both clockwise and anticlockwise directions and are originated periodically. The pressure gradients generated by the vortex shedding induce an alternated force on the body. This force is harmonically variable and perpendicular to the main flow direction. This phenomenon was studied in the past by Kárman, using dimensional analysis on a vibrating cylinder experiment. It was checked the existence of a relation between vortex shedding angular frequency ω_s, the cylinder radius a and the free current velocity U, being that relation denoted by the Strouhal number Sh, defined as $\omega_s a/U$.

The main goal of this article is the analysis of the vibratory motion of a cylinder and a flexible cable when the resonance phenomenon occurs. That means, when the vibration frequency of the cylindrical body equals or gets close to the vortex shedding frequency. The importance of the resonance is given by the fact that in this state of vibration the highest peak-to-peak amplitudes of the cylindrical body displacement are reached. Consequently it leads to the fracture by fatigue in transmission cables.

In the case of a conduction cable, vibration process by the vortexes shedding is more complex. In this case, there is a retroaction between the elastic structure and the air flow by means of a self-damping along the cable. This damping is generated by the friction between the various twisted strings that constitute the cable. When there is resonance, the vibration pattern does not change even with variable wind velocity. The vortex shedding starts being controlled by the vibratory process itself. It is going to be showed later in this article that the cable may have a very dense natural frequency spectrum. This fact raises a lot the chance of the vortex shedding frequency to be equal, or get close, to one of the natural frequencies of the cable, making it to start working in resonance.

2. GOVERNING EQUATIONS

2.1. Governing equation for cable vibration

First consider the free body diagram of a piece of a cable, as shown in Fig. 1.

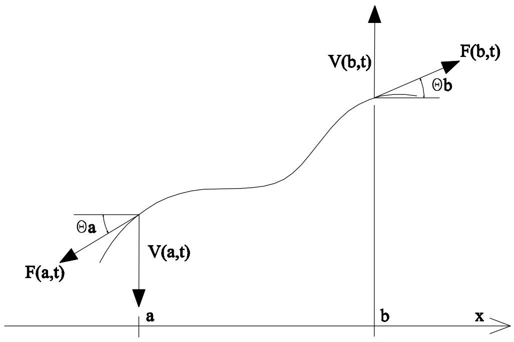

Figure 1. Free body diagram of a non-excited cable

For the governing equation of the vibratory movement of a conduction cable, some hypotheses are taken into account, as it follows:

- The constitutive particles of the cable only have displacement in the *y* direction (transversal vibration);
- The conduction cable has constant transversal section, that is, its inertia moment *I* does not vary in the *x* direction nor with time *t*;
- The conduction cable has constant elasticity module *E*, that is, *E* does not vary in time nor in space;
- The horizontal force *T* is the same force applied to the cable in its ends when they are pinned to poles;
- It is reasonable to assume the *T* force invariant over time;
- The cable linear density γ is homogeneous, that is, $\nabla\gamma = \mathbf{0}$.

A priori, the linear density γ is a function of *t*. However, by the first hypothesis, it is verified that the linear density cannot vary over time.

It is known that the governing equation of a vibrating string is given by (De Figueiredo, 2003):

$$\gamma \frac{\partial^2 y}{\partial t^2} = T \frac{\partial^2 y}{\partial x^2} + F_{ext} \tag{1}$$

where F_{ext} are all the external forces acting over the string, like the aeolian force and the self-damping force, both presented later. A cable, differently of a string, has flectional resistance. Under this condition, the sum of the external forces considered in the balance to get the governing equation takes into account the vertical shear forces *V(x,t)*. Thus, the governing equation for a cable developing a vibratory motion is given by:

$$EI \frac{\partial^4 y}{\partial x^4}(x,t) - T \frac{\partial^2 y}{\partial x^2}(x,t) + \gamma \frac{\partial^2 y}{\partial t^2}(x,t) = F_{ext}(x,y,t) \tag{2}$$

It is proposed in this article an equation for the external aeolian force per length unit F_v, transversal to the flow that acts over a cable. This relation is given by a typical hydrodynamic force:

$$F_v = \rho a U^2 C_L \tag{3}$$

where ρ is the specific mass of the air, *a* is the cable radius, *U* is the non-disturbed flow velocity and C_L is the lifting coefficient.

Oliveira and Freire (1994) proposed a fitting equation for the lifting coefficient C_L based on the equation deductions of Diana and Falco (1971) for a cylinder in vibratory motion. This empirical relation is given by:

$$C_L(\tilde{x},\tau) = \alpha_1 \delta(\tilde{x},\tau) + \alpha_2 \delta^2(\tilde{x},\tau) \tag{4}$$

where δ is the nondimensionalized vibration amplitude of the cable, α_1 and α_2 can be determined by means of experimental data, $\tilde{x}$ and τ are nondimensionalized cable-length position and time variables, respectively.

The self-damping force per length unit (equivalent to the viscous damping force of a mass-spring-damper system), was proposed by Diana *et al* (2000) as being:

$$F_a = C(x,t) \frac{\partial y}{\partial t}(x,t) \tag{5}$$

where *t* is the time, *x* is the position variable along the cable, *y* is the cable transversal displacement and *C(x,t)* is the cable self-damping coefficient.

2.2. Governing equation for cylinder vibration

A simpler system to study and at the same time similar to the cable vibration problem is the concentrated parameters model of a cylinder vibration by the wind. Consider a cylinder of mass m_{cil} as shown in Fig. 2.

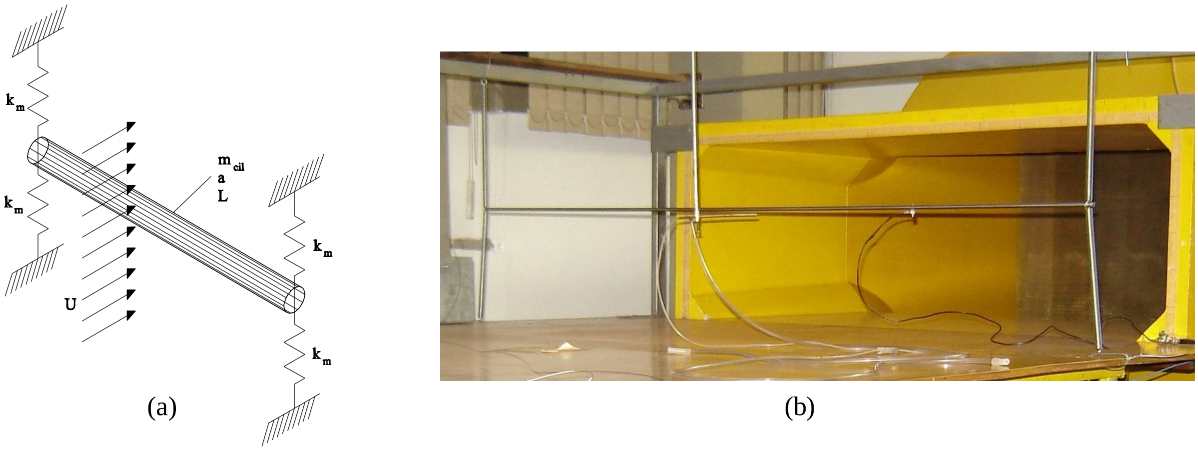

Figure 2. (a) Model of an experimental bench for cylinder vibration experiments, with cylinder aspect ratio *L/a* subjected to a transversal wind flow of velocity *U*. (b) Photo of the cylinder dynamical system used in the experiments. This experimental setup corresponds to the dynamical model shown to the side.

The governing equation for such system can be deduced from a mass-spring-damper system, of concentrated parameters, with variable external force, given by:

$$m\ddot{y} + C\dot{y} + ky = F(t) \tag{6}$$

where $m_{cil} = m$, $4k_m = k$ and the system damping coefficient is $C_{sist} = C$.

Diana and Falco (1971) made several works on this subject, resulting in an equation that describes well the transversal wind force that acts over a cylinder, namely:

$$F(t) = F_0 cos(\Omega t + \phi) \tag{7}$$

F_0 is the aeolian force amplitude, given by:

$$F_0 = \rho L a U^2 C_L \tag{8}$$

where

$$C_L(\tau) = \alpha_0 + \alpha_1 \delta(\tau) + \alpha_2 \delta^2(\tau) \tag{9}$$

The polynomial coefficients also can be determined by experimental data fitting.

3. DIMENSIONAL ANALYSIS

3.1. Dimensional analysis for cylinder vibration

What follows is the nondimensionalization of all the variables involved in the cylinder vibration problem:

$$\delta = y/a \,;\, \tau = \omega_n t \,;\, \frac{C}{m\omega_n} = 2\zeta \,;\, \omega = \frac{\Omega}{\omega_n} \,;\, \omega_0 = \frac{\omega_s}{\omega_n} \tag{10}$$

where ζ is the system damping factor and ω_n is the no-damped system natural frequency.

After a few algebraic manipulations, the governing equation for a vibrating cylinder stands as follows:

$$\frac{d^2\delta}{d\tau^2}+2\zeta\frac{d\delta}{d\tau}+\delta=\left(\frac{\rho La^2}{m}\right)\left(\frac{\omega_s^2}{\omega_n^2}\right)\left(\frac{U^2}{\omega_s^2a^2}\right)C_L(\mathrm{Re},\delta)cos(\omega\tau+\phi) \quad (11)$$

From Equation (11) three physical parameters of the cylinder oscillatory motion can be identified. The first one is the inertia ratio, the second one is the frequencies ratio and the third one, and more important, is the Strouhal number, which is function of the Reynolds number. Thus, it is expected that the cable vibration problem also can be controlled by similar parameters, or even the same ones.

3.2. Dimensional analysis for cable vibration

What follows is the nondimensionalization of all the variables involved in the cable vibration problem. We start defining the following dimensionless quantities:

$$\tilde{x}=x/L \ ; \ \delta=y/a \ ; \ \tau=\omega_n t \quad (12)$$

where ω_n is the free system natural frequency and L is the cable length.

Now the governing equation may be written in terms of the dimensionless quantities, as follows:

$$\frac{EI}{L^2T}\frac{\partial^4\delta}{\partial\tilde{x}^4}(\tilde{x},\tau)-\frac{\partial^2\delta}{\partial\tilde{x}^2}(\tilde{x},\tau)+\frac{\gamma L^2\omega_n^2}{T}\frac{\partial^2\delta}{\partial\tau^2}(\tilde{x},\tau)=\frac{L^2}{aT}\left[F_v(\tilde{x},\tau)+F_a(\tilde{x},\tau)\right] \quad (13)$$

The coefficient of the fourth order derivative term is a nondimensionalized inertia moment *I*, defined as:

$$I^*=\frac{EI}{LT^2}=\frac{E}{T}\left(\frac{2a}{L}\right)^2(2a)^2 \quad (14)$$

It is interesting to notice that, for the inverse aspect ratio *a/L* to be of order of an unit, which is the case in beams vibrations and close to cable pins, *I** has a moderate greatness value, turning the fourth order derivative term to be of great relevance in the governing equation, not being negligible. In the case of having an inverse aspect ratio much lower than the unit, which is the case for long cables, *I** has a weak greatness value, turning the fourth order derivative term negligible in the Eq. (13). In fact, in real applications, the cable length has an order of 102 m, the traction force on the cable pins has an order of 104 N, the elasticity modulus *E* of a cable made mostly of aluminum has an order of 1010 Pa, and for last the cable inertia moment *I* has an order of 10-8 m4, resulting in a coefficient of order 10-6. In this way, it is reasonable to ignore the fourth order derivative term from Eq. (13) in comparison with the other terms of the governing equation.

It is appropriate to define the dimensionless velocity $\tilde{c}$:

$$\tilde{c}=\frac{1}{L\omega_n}\sqrt{\frac{T}{\gamma}} \quad (15)$$

Again, after a few algebraic manipulations, the vibrating cable governing equation reduces to the following dimensionless form:

$$\frac{\partial^2\delta}{\partial\tau^2}-\tilde{c}^2\frac{\partial^2\delta}{\partial\tilde{x}^2}=\frac{1}{\pi}\left(\frac{\rho}{\rho_{cabo}}\right)\left(\frac{1}{Sh^2}\right)\omega_0^2C_L(\mathrm{Re},\delta)+\left(\frac{C}{\gamma\omega_n}\right)\frac{\partial\delta}{\partial\tau} \quad (16)$$

Equation (16) is similar to Eq. (11), except for the self-damping term. It shows that the cylinder vibration problem as well as the cable vibration problem are controlled by important and well-known physical parameters of the system.

Solving the Equation (16) in its homogenous form using the variables separation method, assuming null boundary conditions, it is possible to obtain the cable's non damped free vibration natural frequency, given by:

$$f_n = \frac{n}{2L}\sqrt{\frac{T}{\gamma}} \tag{17}$$

where $n = 1, 2, 3...$ are the vibration harmonics.

4. SOLUTION FOR THE CYLINDER VIBRATION PROBLEM

Substituting Eq. (9) into Eq. (11) we have:

$$\frac{d^2\delta}{d\tau^2} + 2\zeta\frac{d\delta}{d\tau} + \delta = \varepsilon\omega_0^2\left(\alpha_0 + \alpha_1\delta + \alpha_2\delta^2\right)cos(\omega\tau + \phi) \tag{18}$$

where

$$\varepsilon = \frac{\rho L a^2}{m S h^2} \tag{19}$$

The governing equation of the vibratory motion of a cylinder, given by Eq. (18), can be solved analytically using the regular perturbation method. It applies because the ε coefficient has a small value in most practical cases that is used the cylinder model as a simplification of a real system, for instance, vibration of transmission lines (Oliveira, 1989) and offshore structures. For this matter, this article does not take into account restrict cases with high values of ε, where the specific mass of the fluid would be much higher than the vibrating element's.

A resolution of the nonlinear ordinary differential equation by the regular perturbation method consists in determining the solution in a power series form as used by Santos (2005):

$$\delta(\tau) = \delta_0(\tau) + \varepsilon\delta_1(\tau) + \varepsilon^2\delta_2(\tau) + ... = \sum_{j=0}^{n}\varepsilon^n\delta_n(\tau) \tag{20}$$

Substituting Eq. (20) into Eq. (18) and then equating coefficients of like powers of ε, it results in the following set of ordinary differential equation (ODE):

$$\begin{cases} \ddot{\delta}_0 + 2\zeta\dot{\delta}_0 + \delta_0 = 0 \rightarrow O(\varepsilon^0) \\ \ddot{\delta}_1 + 2\zeta\dot{\delta}_1 + \delta_1 = \omega_0^2\left(\alpha_0 + \alpha_1\delta_0 + \alpha_2\delta_0^2\right)\cos(\omega\tau + \phi) = F_1(\tau, \delta_0) \rightarrow O(\varepsilon^1) \\ \ddot{\delta}_2 + 2\zeta\dot{\delta}_2 + \delta_2 = \omega_0^2\left(\alpha_1\delta_0 + 2\alpha_2\delta_0\delta_1\right)\cos(\omega\tau + \phi) = F_2(\tau, \delta_0, \delta_1) \rightarrow O(\varepsilon^2) \\ \vdots \end{cases} \tag{21}$$

The solution of each equation of the system (21) gives the contributions of the solution in Eq. (20). If ε is sufficiently small, which is the case of a cylinder vibratory motion, the term of order ε^2 and higher can be ignored, generating a solution of order $O(\varepsilon^1)$. Thus, for $\varepsilon \mapsto 0$, it is only needed to obtain the solution of the first two equations of the system (21).

The ODE of order ε^0 is the leading order among all the equations in the system and it represents the damped vibration motion of a cylinder. From this equation it is obtained the free damped system natural frequency. In the case of a system with low damping factor, the resonance frequency of the excited system is approximately equal to the natural frequency of the free damped system.

For the solution of the first homogeneous ODE in system (21), we have the following conditions:

$$\zeta < 1 \Rightarrow \delta_0(\tau) = e^{-\zeta\tau}\left[A_1\sin(\sqrt{1-\zeta^2}\tau) + A_2\cos(\sqrt{1-\zeta^2}\tau)\right] \tag{22}$$

$$\zeta = 1 \Rightarrow \delta_0(\tau) = A_1e^{-\tau} + A_2\tau e^{-\tau} \tag{23}$$

$$\zeta > 1 \Rightarrow \delta_0(\tau) = e^{-\zeta\tau}\left(A_1e^{-\sqrt{\zeta^2-1}\tau} + A_2e^{\sqrt{\zeta^2-1}\tau}\right) \tag{24}$$

where A_1 and A_2 are constants obtained from the initial conditions of the cylinder motion.

The second ODE of the system has a forcing term $F_1(\tau,\delta_0)$ that depends of the first ODE solution. From the basic differential equation theory, the second ODE, which is not homogeneous, has a solution as the sum of an homogenous solution and a particular solution, $\delta_1=\delta_{1h}+\delta_{1p}$. The homogenous solution is as similar as the Eqs. (22) to (24). Now for the particular solution, we found:

$$\begin{aligned}\zeta<1\Rightarrow \delta_{1p}(\tau)=&\frac{e^{-\zeta\tau}}{\sqrt{1-\zeta^2}}\sin(\sqrt{1-\zeta^2}\tau)\int_0^\tau F_1(\tau)e^{\zeta\tau}\cos(\sqrt{1-\zeta^2}\tau)d\tau-\\&-\frac{e^{-\zeta\tau}}{\sqrt{1-\zeta^2}}\cos(\sqrt{1-\zeta^2}\tau)\int_0^\tau F_1(\tau)e^{\zeta\tau}\sin(\sqrt{1-\zeta^2}\tau)d\tau\end{aligned} \tag{25}$$

$$\zeta=1\Rightarrow \delta_{1p}(\tau)=-e^{-\tau}\int_0^\tau F_1(\tau)\tau e^{\tau}d\tau+\tau e^{-\tau}\int_0^\tau F_1(\tau)e^{\tau}d\tau \tag{26}$$

$$\zeta>1\Rightarrow \delta_{1p}(\tau)=-\frac{e^{\left(-\zeta-\sqrt{\zeta^2-1}\right)\tau}}{2\sqrt{\zeta^2-1}}\int_0^\tau F_1(\tau)e^{\left(\zeta+\sqrt{\zeta^2-1}\right)\tau}d\tau+\frac{e^{\left(-\zeta+\sqrt{\zeta^2-1}\right)\tau}}{2\sqrt{\zeta^2-1}}\int_0^\tau F_1(\tau)e^{\left(\zeta-\sqrt{\zeta^2-1}\right)\tau}d\tau \tag{27}$$

Using a mathematical software for the several integrations in time, it was possible to obtain the asymptotic solution for the damped resonant ($\omega_0=\omega=1$) motion of a typical cylinder for different values of ε.

Solving Equation (18) numerically, using an adaptive time-step fourth-fifth-order Runge-Kutta method, with algorithm proposed by Press et al (1996), and assuming null initial conditions, that is, static cylinder at start, it was possible to plot the resonant displacement time response of the cylinder, in steady state, for the three damping conditions and two distinct values of ε (the lowest and the highest value tested by the numerical routine). The associate phase diagram $\delta\times\dot{\delta}$ and Fourier transform of the displacement and velocity are also shown in Fig. 3.

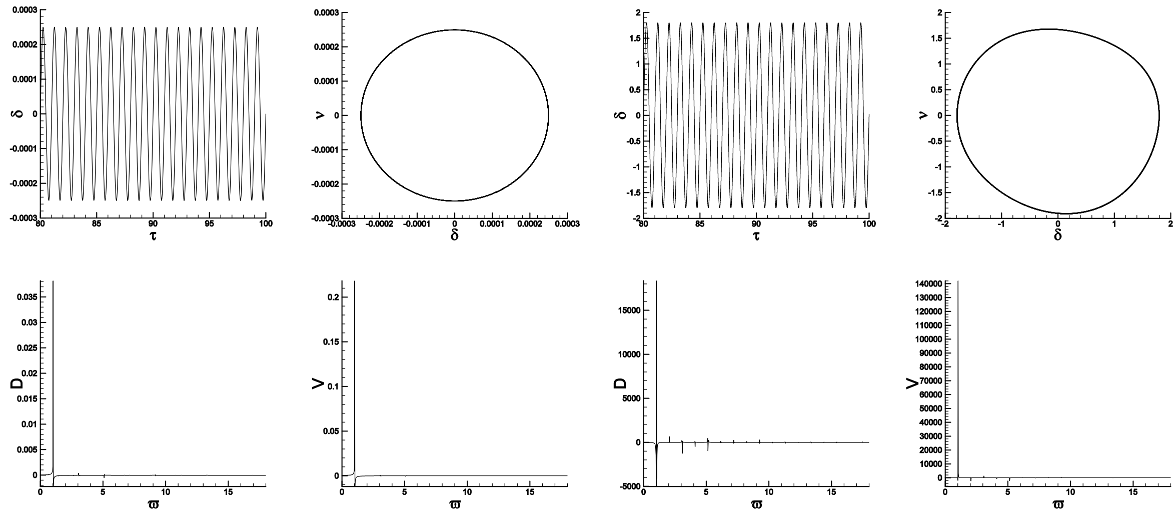

(a) $\varepsilon=0.0001$ (b) $\varepsilon=0.4$

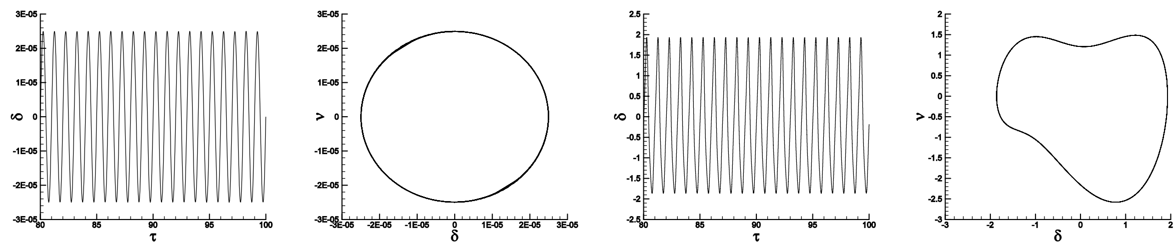

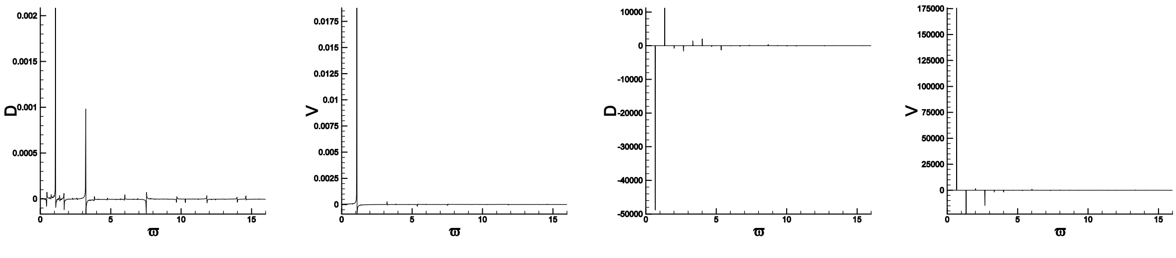

(c) $\varepsilon = 0.0001$ (d) $\varepsilon = 4.7$

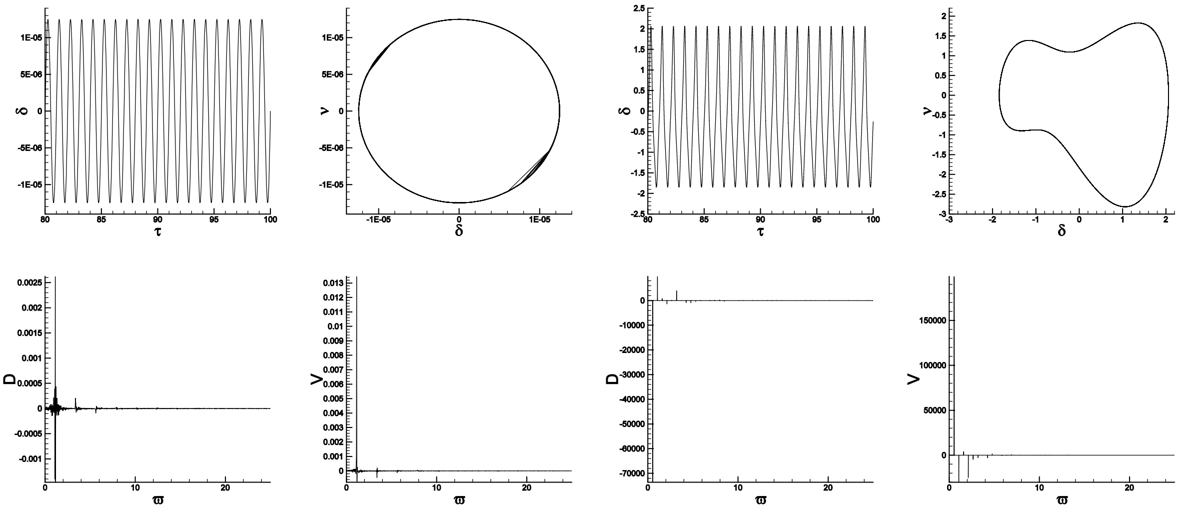

(e) $\varepsilon = 0.0001$ (f) $\varepsilon = 10.0$

Figure 3. Displacement response, phase diagram and FFT of displacement and velocity of a vibrating cylinder in resonant steady state for (a,b) underdamped, (c,d) critical damping and (e,f) overdamped situations.

It can be observed that as ε increases, the nonlinearity in the steady state of the cylinder motion gets more notorious, as shown in the phase diagrams, denoting the decrease in the level of stability of the system. It can also be observed with the increasing of ε that the vibration amplitude on the permanent regime increases significantly. For instance, in overdamped vibration (Fig. 3(e) and 3(f)), the amplitude increases in an order of 105 as ε is increased by 105. It was also possible to notice that the dominant dimensionless frequency is $\varpi \approx 1$ in underdamped systems for any value of ε simulated. This value decreases a little bit (around 0.6) in critical damping and overdamped systems for higher values of ε. Other significant (but not dominant) frequencies start showing up for high-valued ε.

Increasing ε means increasing the air density, increasing the cylinder length, decreasing the cylinder mass or increasing the wind velocity. In an experiment with a wind tunnel size restriction and with not many varieties of fluids, the first two parameters could end up being very hard to be controlled. Thus, in a real experiment, a vibrating cylinder could have a visible vibration steady regime by decreasing its density or increasing the flow velocity in the wind tunnel.

As it can be seen from the plots in Fig. 3, a cylinder does not represent well the vibratory motion of a conduction cable in real application, that is, with low-valued ε. In that case, even with the aeolian excitation force being applied continuously, the cylinder tends to stabilize itself in its equilibrium position after a while, but that is the kind of behavior observed in transmission lines. It is expected that the cable, after a while, comes to a permanent regime vibration because of the continuous wind excitation. Anyway, the illustrative response of the cylinder presented above could be expected because of the typically low greatness level of ε, which could turn the nonlinear term of the ODE negligible. Thus, the vortex-induced-vibration problem with cylinder could become a simple mass-spring-damper system problem.

Figure 4 compares the maximum displacement in steady state of vibration obtained by numerical and asymptotic solutions for different values of ε in the three cases of damping.

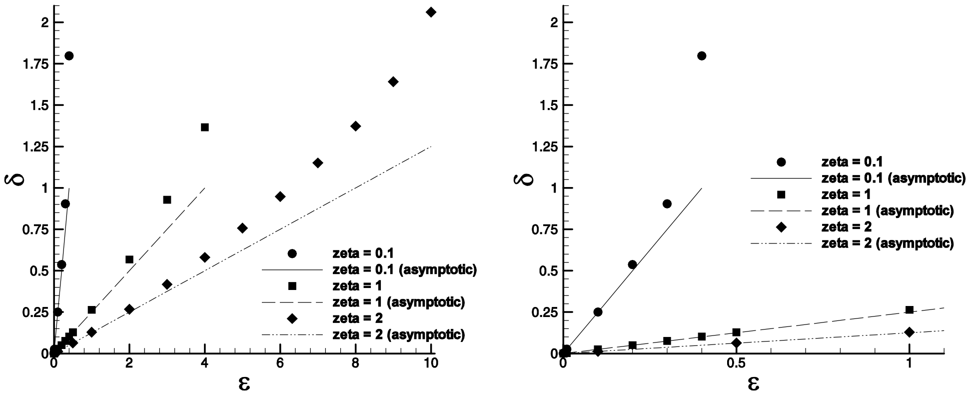

(a) (b)

Figure 4. (a) Maximum displacement of the cylinder in steady regime of vibration for different values of ε . (b) Zoom of plot for lower values of ε .

In Figure 4(a) it is possible to see how the numerical results tend to deviate from the asymptotic solution as ε increases, showing for which values of ε the numerical solution blows up. For instance, accepting an error around 10%, we found that the numerical model gives acceptable results until $\varepsilon = 0.2$ for $\zeta = 0.1$, $\varepsilon = 1$ for $\zeta = 1$ and $\varepsilon = 3$ for $\zeta = 2$. Nevertheless, the numerical solution works fine for low-valued ε , as can be seen in Fig. 4(b), which is a good sign since it shows that the numerical solution gives trustable results for most practical cases in engineering.

5. SOLUTION FOR THE CABLE VIBRATION PROBLEM

5.1. Analytical solution

Substituting Eq. (4) and Eq. (19) into Eq. (16) we have the extended wave equation:

$$\frac{\partial^2 \delta}{\partial \tau^2} - \tilde{c}^2 \frac{\partial^2 \delta}{\partial \tilde{x}^2} = \varepsilon \omega_0^2 \left[\alpha_1 \delta(\tilde{x},\tau) + \alpha_2 \delta^2(\tilde{x},\tau) \right] + \left(\frac{C}{\gamma \omega_n} \right) \frac{\partial \delta}{\partial \tau} \tag{28}$$

Assuming the self-damping coefficient to be constant in time (which is not true for real cases), Eq. (28) was solved numerically using an implicit finite difference method.

The program was supposed to be validated by comparing its results with an analytical solution of the cable vibration problem. However, the quadratic term of the lifting coefficient turns the wave equation to be nonlinear, making it hard to obtain an analytical solution. Because of that, the validation of the program was made by comparing the numerical solution of the extended wave equation assuming the lifting coefficient not to be quadratic, but linear.

The cable vibration problem was simplified, for validation, to the following:

$$\begin{cases} \dfrac{\partial^2 \delta}{\partial \tau^2} - \tilde{c}^2 \dfrac{\partial^2 \delta}{\partial \tilde{x}^2} = \varepsilon \omega_0^2 \alpha_1 \delta(\tilde{x},\tau) + \left(\dfrac{C}{\gamma \omega_n} \right) \dfrac{\partial \delta}{\partial \tau} \\ \delta(0,\tau) = \delta(1,\tau) = 0 \\ \delta(\tilde{x},0) = \dfrac{\gamma g L^2}{2Ta} \left(\tilde{x}^2 - \tilde{x} \right) \\ \dfrac{\partial \delta}{\partial \tau}(\tilde{x},0) = 0 \end{cases} \tag{29}$$

where the initial condition is a simplification of the shape of a suspended cable proposed by Labegalini et al (1992).

Using the variables separation method, the obtained general solutions of Eq. (29) are the following:

$$\delta(\tilde{x},\tau) = \sum_{n=1}^{\infty} A_{1n} e^{\frac{B}{2}\tau} \left[e^{-\frac{\varphi_{1n}}{2}\tau} - \left(\frac{B - \varphi_{1n}}{B + \varphi_{1n}} \right) e^{\frac{\varphi_{1n}}{2}\tau} \right] \sin(n\pi \tilde{x}) \tag{30}$$

$$\delta(\tilde{x},\tau)=\sum_{n=1}^{\infty}A_{2n}e^{\frac{B}{2}\tau}\left[\sin\left(\frac{\varphi_{2n}}{2}\tau\right)-\frac{\varphi_{2n}}{B}\cos\left(\frac{\varphi_{2n}}{2}\tau\right)\right]\sin(n\pi\tilde{x}) \tag{31}$$

where

$$B=\frac{C}{\gamma\omega_n}\ ,\ \varphi_{1n}=\sqrt{B^2+4\left(\varepsilon\omega_0^2\alpha_1-n^2\pi^2\tilde{c}^2\right)}\ ,\ \varphi_{2n}=\sqrt{-\left[B^2+4\left(\varepsilon\omega_0^2\alpha_1-n^2\pi^2\tilde{c}^2\right)\right]}$$

and the Fourier coefficients are

$$A_{1n}=\left(\frac{B+\varphi_{1n}}{2\varphi_{1n}}\right)\left(\frac{2}{n^3\pi^3}\right)\left(\frac{\gamma gL^2}{Ta}\right)\left[(-1)^n-1\right]$$

$$A_{2n}=\left(-\frac{B}{\varphi_{2n}}\right)\left(\frac{2}{n^3\pi^3}\right)\left(\frac{\gamma gL^2}{Ta}\right)\left[(-1)^n-1\right]$$

The solution shown in Eq. (30) is for the case $B^2+4\left(\varepsilon\omega_0^2\alpha_1-n^2\pi^2\tilde{c}^2\right)>0$ and the solution shown in Eq. (31) is for the case $B^2+4\left(\varepsilon\omega_0^2\alpha_1-n^2\pi^2\tilde{c}^2\right)<0$.

5.2 Numerical solution

The Equation (28) can be rewritten as:

$$\frac{\partial^2\delta}{\partial\tau^2}-\tilde{c}^2\frac{\partial^2\delta}{\partial\tilde{x}^2}-A\alpha_1\delta(\tilde{x},\tau)-A\alpha_2\delta^2(\tilde{x},\tau)-B\frac{\partial\delta}{\partial\tau}=0 \tag{32}$$

where $A=\varepsilon\omega_0^2$ and B is a nondimensionalized self-damping coefficient, as defined for Eqs. (30) and (31).

We use a time-centered implicit differencing method, presented by Tannehill et al (1997) as Crank-Nicolson differencing, in order to evade instability matters. Thus, we have the following differential representations:

$$\frac{\partial^2\delta}{\partial\tau^2}=\frac{\delta(\tilde{x}_0,\tau_0+\Delta\tau)+\delta(\tilde{x}_0,\tau_0-\Delta\tau)-2\delta(\tilde{x}_0,\tau_0)}{\Delta\tau^2} \tag{33}$$

$$\frac{\partial\delta}{\partial\tau}=\frac{\delta(\tilde{x}_0,\tau_0+\Delta\tau)-\delta(\tilde{x}_0,\tau_0-\Delta\tau)}{2\Delta\tau} \tag{34}$$

$$\frac{\partial^2\delta}{\partial\tilde{x}^2}=\frac{\delta(\tilde{x}_0+\Delta\tilde{x},\tau_0+\Delta\tau)+\delta(\tilde{x}_0-\Delta\tilde{x},\tau_0+\Delta\tau)-2\delta(\tilde{x}_0,\tau_0+\Delta\tau)}{\Delta\tilde{x}^2} \tag{35}$$

where $\Delta\tilde{x}$ and $\Delta\tau$ are, respectively, the differential in nondimensionalized space and time. Substituting Equations (33) through (35) into Eq. (32), we obtain:

$$\left(\frac{1}{\Delta\tau^2}\right)\delta(\tilde{x}_0,\tau_0+\Delta\tau)+\left(\frac{1}{\Delta\tau^2}\right)\delta(\tilde{x}_0,\tau_0-\Delta\tau)+\left(-\frac{2}{\Delta\tau^2}\right)\delta(\tilde{x}_0,\tau_0)+$$
$$+\left(-\frac{\tilde{c}^2}{\Delta\tilde{x}^2}\right)\delta(\tilde{x}_0+\Delta\tilde{x},\tau_0+\Delta\tau)+\left(-\frac{\tilde{c}^2}{\Delta\tilde{x}^2}\right)\delta(\tilde{x}_0-\Delta\tilde{x},\tau_0+\Delta\tau)+$$
$$+\left(\frac{2\tilde{c}^2}{\Delta\tilde{x}^2}\right)\delta(\tilde{x}_0,\tau_0+\Delta\tau)-A\alpha_1\delta(\tilde{x}_0,\tau_0+\Delta\tau)-A\alpha_2\delta^2(\tilde{x}_0,\tau_0+\Delta\tau)+ \quad (36)$$
$$+\left(-\frac{B}{2\Delta\tau}\right)\delta(\tilde{x}_0,\tau_0+\Delta\tau)+\left(\frac{B}{2\Delta\tau}\right)\delta(\tilde{x}_0,\tau_0-\Delta\tau)=0$$

Organizing Equation (36) by allocating like terms, we obtain:

$$\left(-\frac{\tilde{c}^2}{\Delta\tilde{x}^2}\right)\delta(\tilde{x}_0-\Delta\tilde{x},\tau_0+\Delta\tau)+\left(\frac{1}{\Delta\tau^2}+\frac{2\tilde{c}^2}{\Delta\tilde{x}^2}-A\alpha_1-\frac{B}{2\Delta\tau}\right)\delta(\tilde{x}_0,\tau_0+\Delta\tau)+$$
$$+(-A\alpha_2)\delta^2(\tilde{x}_0,\tau_0+\Delta\tau)+\left(-\frac{\tilde{c}^2}{\Delta\tilde{x}^2}\right)\delta(\tilde{x}_0+\Delta\tilde{x},\tau_0+\Delta\tau)+ \quad (37)$$
$$+\left(\frac{1}{\Delta\tau^2}+\frac{B}{2\Delta\tau}\right)\delta(\tilde{x}_0,\tau_0-\Delta\tau)+\left(-\frac{2}{\Delta\tau^2}\right)\delta(\tilde{x}_0,\tau_0)=0$$

Replacing each ($\tilde{x}_0,\tau_0$) node in the space-time grid by the *i-j* notation, we obtain the following finite difference discrete equation:

$$A_1\delta_{i-1}^{j+1}+A_2\delta_i^{j+1}+A_5\left(\delta_i^{j+1}\right)^2+A_1\delta_{i+1}^{j+1}+A_3\delta_i^{j-1}+A_4\delta_i^{j}=0 \quad (38)$$

where

$$A_1=-\frac{\tilde{c}^2}{\Delta\tilde{x}^2}$$

$$A_2=\frac{1}{\Delta\tau^2}+\frac{2\tilde{c}^2}{\Delta\tilde{x}^2}-A\alpha_1-\frac{B}{2\Delta\tau}$$

$$A_3=\frac{1}{\Delta\tau^2}+\frac{B}{2\Delta\tau}$$

$$A_4=-\frac{2}{\Delta\tau^2}$$

$$A_5=-A\alpha_2$$

For each iteration *j+1* in time, it is used the classical method of Newton, presented by Ruggiero and Lopes (1996), to solve the set of nonlinear equations, that can be written as a vector, with *i* components, of nonlinear multivariable functions $F(\delta_i^{j+1})=0$ from Eq. (38). Since it is easy to see that the Jacobian of $F(\delta_i^{j+1})$ is a tridiagonal linear matrix, the classical Thomas algorithm is implemented inside the Newton method solver.

The numerical solution obtained by the program for the problem proposed in (29) is consistent to the analytical solution in (30) and (31), as it was verified in animations of the vibrating cable, thus confirming the validation of the computational routine.

However, both solutions tend to the infinite for high temporal values, as it can be seen in Fig. 5.

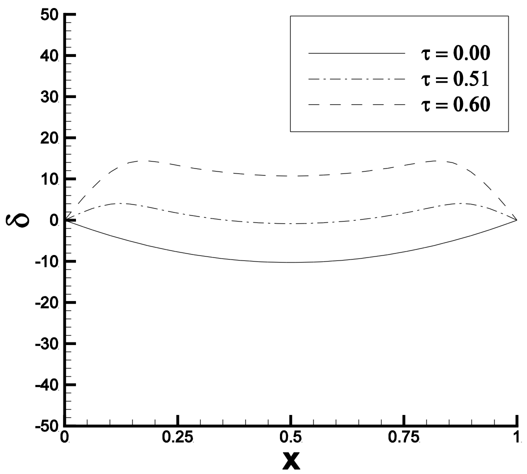

Figure 5. Simulation of break up of cable for $\tau > 0.5$.

As it can be noticed from Eqs. (30) and (31), the responsible for this "explosion" of the time response is an exponential temporal function with coefficient *B*, which is function of the self-damping coefficient *C*. As expected from an exponential function, it assumes greater values for greater times. Thus, we can conclude that considering the self-damping coefficient *C* to be constant in time is not a good hypothesis for the solution of the cable vibration problem.

Even so, the computational routine for the finite difference problem with nonlinear wind force works fine and is ready to load time data of $C(\tau)$, that can be obtained from experiments of real cables, in order to be used in each time iteration of the program.

6. CONCLUSIONS

The presented work has been focused firstly on the nondimensionalization of the governing equations for both cylinder and cable vibration problems. The cylinder vibration problem was analyzed by using a regular perturbation method in order to solve the governing equation and by plots of time responses of a typical cylinder for different values of the weak-term constant ε. Those results have shown that a cylinder can have a balanced pattern of vibration for small values of ε, but this balance is lost once ε is increased, that means, a possible high order of nonlinearity in this fluid-structure problem may cause the structure to eventually collapse.

The cable vibration problem was analyzed by solving numerically the proposed extended wave equation with its initial boundary and initial conditions. In order to validate the computational program that simulates the cable vibration, it was assumed the hypothesis of linear lifting coefficient and constant self-damping coefficient. In the validation and for the real case of quadratic lifting coefficient, the solution tended to infinite, due to the consideration of constant self-damping coefficient. However, the program showed to work fine and its routine is ready for loading of time data of the self-damping coefficient that can be obtained from experiments with real cables.

7. REFERENCES

Batchelor, G.K., 1967, "An introduction to fluid dynamics", Cambridge University Press, Cambridge.

Diana, G. and Falco, M., 1971, "On the forces transmitted to a vibrating cylinder by a blowing fluid", Meccanica, Vol. VI, No 1, pp. 9-22.

Diana, G., Falco, M., Cigada, A. and Manenti, A., 2000, "On the measurement of over head transmission lines conductor self-damping", IEEE Transactions on Power Delivery, Vol. 15, No 1, pp. 285-292.

Figueiredo, D.G., 2003, "Análise de Fourier e equações diferenciais parciais", Ed. Edgard Blücher, S. Paulo, Brazil, 274p.

Labegalini, P.R., Labegalini, J.A., Fuchs, R.D., Almeida, M.T., 1992, "Projetos mecânicos das linhas aéreas de transmissão", Ed. Edgard Blücher, S. Paulo, Brazil, 528 p.

Oliveira, A.R.E., 1989, "A mathematical model for wind-induced oscillations of cylindrical structures", VI International Conference on Numerical Methods in Laminar and Turbulent Flow, Swansea, Wales, U.K.

Oliveira, A.R.E. and Freire, D.G., 1994, "Dynamical modelling and analysis of aeolian vibrations of single conductors", IEEE Transactions on Power Delivery, Vol. 9, No 3, pp. 1685-1693.

Press, W.H., Teukolsky, S.A., Vetterling, W.T., Flannery, B.P., 1996, “Numerical recipes in Fortran 90 – The art of parallel scientific computing”, Cambridge University Press, New York, U.S.A., 1486 p.
Ruggiero, M.A.G., Lopes, V.L.R., 1996, “Cálculo numérico – aspectos teóricos e computacionais”, 2nd edition, Ed. Makron Books, S. Paulo, Brazil, 406 p.
Santos, R.A.M., 2005, “Comportamento dinâmico de bolhas em fluidos complexos”, Master’s thesis, DM-085, Universidade de Brasília, Brasília, Brasil.
Tannehill, J.C., Anderson, D.A., Pletcher, R.H., 1997, “Computational Fluid Mechanics and Heat Transfer”, 2nd edition, Taylor & Francis Publishers, Philadelphia, U.S.A., 792 p.

8. RESPONSIBILITY NOTICE

The authors are the only responsible for the printed material included in this paper.